Analyst

ROYAL SOCIETY OF CHEMISTRY

PAPER

View Article Online
View Journal | View Issue

Cite this: *Analyst*, 2022, **147**, 4517

Dual-mode ion-selective electrodes and distance-based microfluidic device for detection of multiple urinary electrolytes†

Kamonchanok Phoonsawat,[a,b,c] Tugba Ozer, *[d] Wijitar Dungchai [a] and Charles S. Henry *[c,e,f]

Here, we developed a microfluidic paper device by combining ion-selective electrodes (ISE) and a distance-based paper device (dPAD) for simultaneous potentiometric and colorimetric detection of urine electrolytes including K^+, Na^+ and Cl^-. The working and reference electrode zones were coated with polystyrene as a non-ionic polymer to improve hydrophobic properties on the paper surface for fabrication of K^+-ISE and Na^+-ISE. The layer of polymer coating was optimized to enhance the sensitivity of the ISEs. Under optimized conditions, the electrode surfaces were modified with carbon black to improve the electrochemical characteristics of the ISEs. The ISEs showed good performance with sensitivities of 54.14 ± 3.94 mV per decade and 55.08 ± 1.15 mV per decade for K^+ and Na^+ within the linear concentration range 0.100 mM–100 mM K^+ and 5 mM–1 M Na^+, respectively. The limits of detection (LOD) were 0.05 mM and 1.36 mM for K^+ and Na^+, respectively. The linear working range of Cl^- was 0.50 to 50 mM and the LOD and limit of quantification (LOQ) were found to be 0.16 ± 0.05 mM (3SD) and 0.53 ± 0.05 mM (10SD), respectively. The dual-mode ISE-dPAD was validated in human urine and recoveries were obtained as 90–108%, 94–105%, and 90–96% for K^+, Na^+, and Cl^-, respectively, showing successful application of the developed device in a complex matrix. The ISE-dPAD has advantages including low-cost ($ 0.33 per test), eco-friendly, portability, simple operation, the need of low sample volume (100 μL), and simultaneous analysis on a single device.

Received 25th July 2022,
Accepted 5th September 2022

DOI: 10.1039/d2an01220k

rsc.li/analyst

Introduction

Urine electrolytes, Na^+, K^+, and Cl^-, are used to diagnose various disorders such as cardiovascular diseases, hyperkalemia or hypokalemia, kidney disease or injury, adrenal gland problems, rickets, hypothyroidism, steatorrhea, vitamin D overdose, and renal tubular acidosis.[1–3] Physiologically, the effects of Na^+ and K^+ are intertwined in the body, and inadequate K^+ consumption is linked to high blood pressure.[4] In addition, Cl^- levels are used to diagnose cystic fibrosis and diabetic acidosis.[2] In recent years, the Na : K ratio has been suggested as a more reliable index to assess the risk of hypertension (HTN) and cardiovascular diseases (CVD).[5–7] However, a ratio of <1.0 has been identified as the best balance of Na^+ and K^+ intakes for preventing CVD and all-cause mortality.[8] The determination of 24-hour urinary electrolyte excretion is commonly used to evaluate dietary group intakes of the salt in food, which has critical implications for numerous diseases and health concerns.[9] Thus, quantitative detection of 24-hour urinary Na^+, K^+, and Cl^- is important for monitoring of health conditions. The traditional methods for sensitive and selective analysis of these electrolytes are ion chromatography,[10,11] surface plasmon resonance,[12] and inductively coupled plasma mass spectrometry.[13,14] However, expensive and bulky instruments, specialized personnel and high volume of samples are necessary for performing these methods to quantify target analytes. On the other hand, point-of-care (POC) monitoring is a growing need to develop electrolyte sensing systems that use miniaturized portable devices and microliter sample volumes for biomedical applications.

Colorimetric and electrochemical detection methods are the most commonly used with microfluidic paper-based

[a]*Organic Synthesis, Electrochemistry & Natural Product Research Unit, Department of Chemistry, Faculty of Science, King Mongkut's University of Technology Thonburi, Bangkok, 10140, Thailand*
[b]*Engineering Science Classroom, Darunsikkhalai School, King Mongkut's University of Technology Thonburi, Bangkok, 10140, Thailand*
[c]*Department of Chemistry, Colorado State University, Fort Collins, CO 80523, USA*
[d]*Department of Bioengineering, Faculty of Chemical-Metallurgical Engineering, Yildiz Technical University, 34220 Istanbul, Turkey. E-mail: tozer@yildiz.edu.tr*
[e]*School of Biomedical Engineering, Colorado State University, Fort Collins, Colorado 80523, USA*
[f]*Metallurgy and Materials Science Research Institute, Chulalongkorn University, Bangkok, Thailand. E-mail: Chuck.Henry@colostate.edu*

†Electronic supplementary information (ESI) available: Estimated device cost per test, the potentiometric response to the conditioned times and effect of carbon black, the effect of pH, selectivity assay, water layer tests, and storage times of device. See DOI: https://doi.org/10.1039/d2an01220k

analytical devices (μPADs) for analysis due to their simplicity, low-cost and portability. Due to the presence of fibers, paper is a great platform to store chemicals and (bio)reagents.[15,16] Paper-based electrochemical analytical devices have been developed for potentiometric ion-selective sensing in recent years.[17] Ion-selective electrodes (ISEs) have been widely used to determine electrolytes in biological samples since they are simple to fabricate, user-friendly, low-cost, portable, and can be used without sample pretreatment.[18] Some attempts have been made to develop μPAD-based ISEs for quantification of K^+ and Na^+ as single analytes[19,20] and simultaneously.[21,22] For example, Cao *et al.* have recently reported a μPAD patch containing screen-printed ISEs layer for monitoring K^+ and Na^+ in perspiration.[23] In another report, μPAD was developed for potentiometric determination of K^+, Na^+, Ca^{2+} and Cl^- by Lan *et al.*[24] Although, the ions could be detected using a small volume (<10 μL) of sample, the cation selective electrodes showed the lower slopes of the calibration curves than their theoretical whereas the Cl^--ISE had super Nernstian response with a slope of −61.8 ± 1.0 mV per decade. In addition, the potentiometric reading resulted in more than 10% relative error, which is larger than that of the conventional measurements. Ding *et al.* presented a gold-modified paper for potentiometric detection of K^+, Na^+ and Cl^- in clinical samples.[25] PEDOT(PSS) and PEDOT(Cl) were electrochemically deposited on electrode surface as the ion-to-electron transducer for fabrication of solid-contact ISEs. It was observed that the modification of the paper substrates with gold nanoparticles improved the accuracy of the ISEs in samples. However, AuNPs synthesis and an external reference electrode are needed for employing this device. Therefore, these limitations should be overcome for a simultaneous detection of Na^+, K^+, and Cl^- while generating minimal waste for biological analysis.

The dual-mode sensing with colorimetric detection and electrochemical detection using cyclic voltammetry on a μPAD has been demonstrated in several works for environmental and criminal applications.[26,27] Likewise, colorimetric and electrochemical detection can be accompanied each other to allow highly sensitive analysis of various ions that cannot be detected by a color change for clinical applications to extend the working range for ion of interest. In a recent work, potentiometric K^+-ISE on transparency polyethylene terephthalate (PET) substrate using in-house stencil printing method and paper-based device was combined.[28] However, this device contains three layers of PET and double-side stacking tape, which increase the device costs and fabrication steps. Therefore, we decided to use a paper substrate, which is inexpensive and widely available, to fabricate the combined device. On the other hand, due to porous structure and the electrostatic interaction between cations in samples and carboxyl/hydroxyl groups on paper substrate, μPADs are not able to work well for sensitive and accurate potentiometric detection of ions using ISEs.[29] To overcome this issue, hydrophobic polymers, such as polyethylene, polystyrene, and polyvinylchloride, can be coated on paper materials to provide hydrophobicity for fabrication of ISEs.[30] Therefore, we chose polystyrene as the hydrophobic polymer to modify the paper substrate for fabrication of the dual ISEs due the lack of ionic charges on the polymer since they can electrostatically interact with primary ions in the analyte, resulting in false signals.

Here, a paper substrate was engineered to develop a dual-mode device including K^+-ISE and Na^+-ISE for potentiometric detection and a distance-based paper device (dPAD) for colorimetric Cl^- detection for the first time. Laser engraving was used to generate a microchannel for the dPAD to allow sample flow, and wax printing was used to form barriers for the ISEs. Based on the device design, there is no need to use adhesive tape to attach compared to the existing dual devices in the literature.[27,31] A three-electrode cell configuration including two working electrodes and a reference electrode was used for potentiometric detection of K^+ and Na^+ ions. The paper for ISE area was coated with polystyrene as the non-ionic polymer to provide hydrophobic properties. Then, the electrodes were fabricated *via* screen printing. The electrodes were modified with carbon black to improve sensitivity. While the potentiometric responses were measured using a portable potentiostat, Cl^- detection was performed instrument-free. The dual-ISE could selectively detect K^+ and Na^+ with sensitivities of 54.14 ± 3.94 and 55.08 ± 1.15 mV per decade for K^+ and Na^+, respectively. The dual-ISE-dPAD was applied for simultaneous electrolyte detection in human pooled urine as a proof-of-concept. To the best of our knowledge, this is the first report that potentiometric and distanced-based colorimetric detection strategies are performed simultaneously on a single device.

Experimental

Materials and instruments

Sodium tetrakis-[3,5-bis(trifluoromethyl)phenyl]borate (NaTFPB), sodium ionophore I, potassium tetrakis(4-chlorophenyl) borate (KTClPB, >98%), potassium ionophore I, bis(2-ethylhexyl) sebacate (DOS, >97%), poly(butyl methacrylate-*co*-methyl methacrylate), tetradodecylammonium tetrakis(4-chlorophenyl)borate, high molecular weight polyvinyl chloride (PVC), D-glucose, sucrose, and 4-(2-hydroxyethyl) piperazine-1-ethanesulfonic acid (HEPES), polystyrene (45 000), dichloromethane were obtained from Sigma-Aldrich. Tetrahydrofuran (THF) from Sigma-Aldrich was freshly distilled before use. Vulcan XCMAX22 carbon black was obtained from Cabot Corporation (Boston, USA). $AgNO_3$, K_2CrO_7, NaCl, $NaNO_3$, KCl, KNO_3, $MgCl_2$, $CaCl_2$, $NaHCO_3$, and NaH_2PO_4 were analytical grade and purchased from Fisher Scientific. The human pooled urine was purchased from Lee BioSolutions Inc. and spiked with standard K^+, Na^+, and Cl^- for sample analysis. No IRB approval was required for this work because it used deidentified, banked samples. All aqueous solutions were prepared with Milli-Q water (18.2 MΩ cm). Whatman No. 4 filter paper was purchased from Cole-Parmer (VernonHills, IL). Laser cutting was performed using an Epilog Laser Cutter (Golden, CO).

Morphological characterization of modified paper substrate

The morphology of the polystyrene-modified and unmodified paper substrates was analyzed using JSM-7600 Field Emission Scanning Electron Microscopy (FE-SEM) (Japan). The paper was modified with one layer, two layers, and three layers of polystyrene (0.1 g L^{-1} in dichloromethane), whereas some devices were left unmodified for comparison.

Preparation of ion-selective membranes

According to our previous procedure, the ion-selective membranes (ISM) for fabrication of Na^+-ISE and K^+-ISE were prepared.[32,33] While 2% (w/w) of sodium ionophore I, 0.5% (w/w) of NaTCPB, 65% (w/w) of DOS, and 32.5% (w/w) of PVC were mixed in 2 mL THF for Na^+-ISM, 2% (w/w) of potassium ionophore I, 0.6% (w/w) of KTCPB, 64.7% (w/w) of DOS, and 32.7% (w/w) of PVC were mixed in 1.5 mL THF for the preparation K^+-ISM. 200 mg of the reference electrode membrane consists of 73% (w/w) of poly(butyl methacrylate-*co*-methyl methacrylate), 25% (w/w) of KCl, and 2% (w/w) of tetradodecyammonium tetrakis (4-chlorophenyl) borate were mixed in 1 mL THF and sonicated for 15 min to prepare reference electrode membrane. 5 mg mL^{-1} carbon black (Vulcan XCmax, Cabot Corporation) dispersion was prepared in THF and sonicated for 15 min to modify working electrode surfaces.

Architecture and fabrication of the device (ISE-dPAD)

The dual ion-selective electrodes combined with dPAD consists of a Na^+-ISE channel, a K^+-ISE channel, a reference channel for potentiometric detection, and a Cl^- channel for distance-based colorimetric detection is presented in Fig. 1. The device, which consists of a connection area (3 × 5 mm) to the sample inlet and ISE zone (25 × 55 mm), a circular well (diameter 7 mm), and a flow channel (3 × 30 mm) for the Cl^- test zone, was designed using CorelDraw software and printed on the Whatman No. 4 filter paper with a wax printer to define barriers and accommodate electrodes. The wax was melted through the paper by heating on a hotplate at 120 °C for 5 min. After printing, the ISE area was coated with two layers (50 μL × 2 aliquots) of polystyrene by a paintbrush and allowed to dry at room temperature. The electrode pattern was designed using CorelDraw software and applied on a polyethylene terephthalate (PET) sheet by using a CO_2 laser cutter. The mixture of 1 g carbon ink (E3178, Ercon Inc., Massachusetts, USA) and 0.6 g of TC303 graphite (20 μm, Asbury Carbons, New Jersey, USA) was printed on polystyrene modified filter paper *via* in-house screen-printed method for fabrication of working electrodes and a solid-state reference electrode (RE). Next, the electrodes were placed in an oven at 60 °C for 30 min. Next, Ag/AgCl ink was applied on the reference electrode zone and cured at 60 °C for 10 min. After the fabricated device was allowed to cool down to room temperature and its backside was covered with a packing tape to prevent solution leakage during sample analysis. The reference electrode zone was coated with three aliquots (2 μL × 3) of reference membrane whereas Na^+-ISE and K^+-ISE zones were modified with carbon black in two (1.5 μL × 2), and Na^+-ISM and K^+-ISM in three aliquots (2 μL × 3), respectively. Finally, the ISM coated electrodes were left in a desiccator for overnight to evaporate the residual solvent. For dPAD testing, reagents including 50 mM $AgNO_3$ (5 μL) and 25 mM $K_2Cr_2O_7$ (5 μL) were spotted onto the detection zone and allowed to dry at room temperature before use.

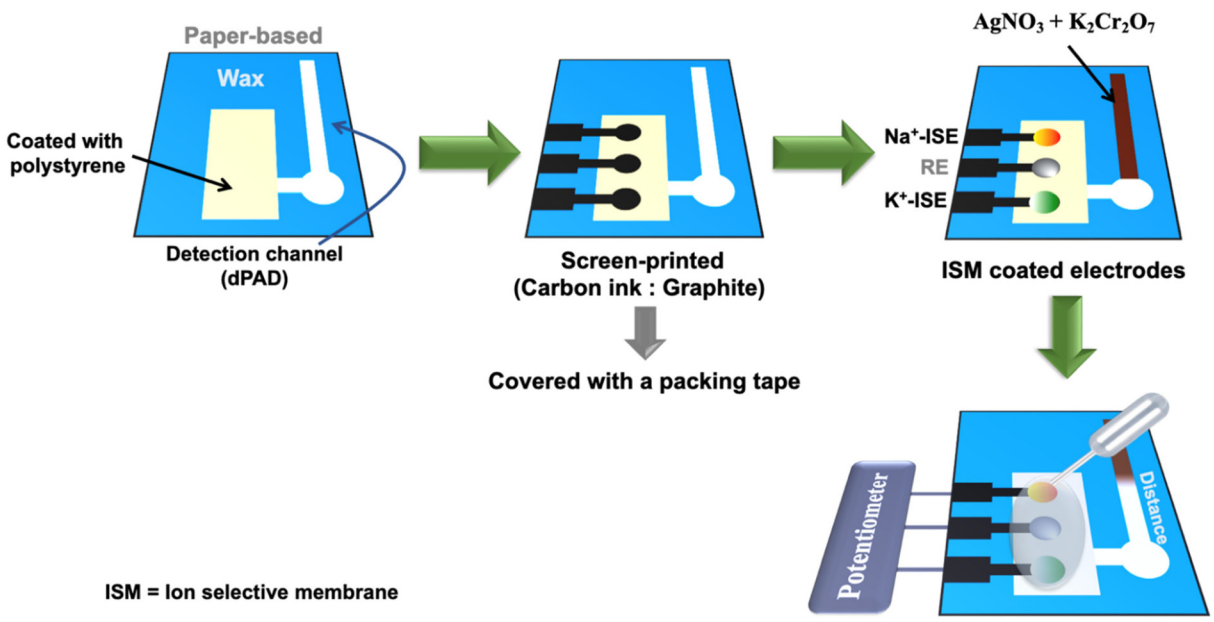

Fig. 1 Schematic illustration of simultaneous K^+ and Na^+ detection on the ion-selective electrode (ISE) and Cl^- detection on the distance-based paper device (dPAD).

Electrolyte detections on the dual-ISE-dPAD

The activities of K^+ and Na^+ were measured with a WiFi-supported portable electrochemical analyzer (Palmsens) in the presence of three-electrode system including two working ISEs and an all-solid-state reference electrode. The activity coefficients were calculated by the Debye–Hückel equation.[34] In addition, cyclic voltammetry measurements were performed by the electrochemical analyzer using three-electrode system including a working electrode, a counter and a reference electrode. All measurements were performed at room temperature (23 ± 2 °C). According to our previous work, the Cl^- content in samples was determined by measuring the formation of white color band length appeared after Cl^- was reacted with reagents in the dPAD area. The cost of the dual-mode hetero-sensing device is about $0.33 per test (Table S1†).

Results and discussion

The device operation

The developed dual mode PAD consists of two components, a dPAD for colorimetric detection of Cl^- and an electrochemical PAD (ePAD) for potentiometric detection of Na^+ and K^+. These hybrid sensing modes were designed to achieve wide linear ranges and facilitate each sensing concept for electrolyte determination. Due to micropatterning of the flow channel of the dPAD *via* etching using a laser engraving machine, the capillary flow rate was improved, making the device suitable for the viscous samples.[35] The device is shown in Fig. 1. The Cl^- was detected by dPAD using the reaction between silver nitrate ($AgNO_3$), potassium dichromate ($K_2Cr_2O_7$), and Cl^- according to our previous work.[36] Once the Cl^- was added to the sample zone and reacted with the reagent, the AgCl precipitation is formed in the detection zone and the color changed from brown to white. The length of the color band changing from the background is related to the Cl^- concentration. The reaction between Cl^- and $Ag_2Cr_2O_7$ on the detection channel is shown in the reaction (1).

$$Ag_2Cr_2O_7 + 2KCl \rightarrow 2AgCl + K_2Cr_2O_7 \quad (1)$$

Optimization of the polymer coated layers on the electrode area

ISEs based on hydrophobic ISM are typically made of a plasticized polymer that forms an organic membrane phase that is immiscible with the aqueous sample.[30] Paper has hydrophilic properties, so polystyrene was used to coat paper substrate to provide hydrophobicity. Polystyrene as a non-ionic polymer was chosen for coating the ISE zone since they do not contain charges that can adversely affect potentiometric detection.[37] However, the number of polymer coating layers is important for electrode fabrication. Therefore, the ISE performances were evaluated by varying number of polymer coating layers including one, two, three, and four layers on the electrode area *via* electrochemical characterization. Potentiometric responses of the ISEs in the presence of varying polymer layer was presented in Table 1. It was concluded that the two layers of the polymer coating gave the best sensitivity with a slope of 54.40 ± 0.67 mV per decade for K^+, which is in agreement other observations for conducting polymers such as PEDOT used for similar K-ISEs.[38]

Table 1 Potentiometric response to the number of polymer coating layers on the electrode area (n = 4)

Target ion	Number of layers	Slope (mV per decade)
K^+	0	20.50 ± 2.50
	1	48.69 ± 0.77
	2	54.40 ± 0.67
	3	48.45 ± 1.05
	4	46.19 ± 0.68

The morphology of the polystyrene modified, and unmodified paper substrate was investigated by SEM analysis and the images are shown Fig. 2. The polystyrene modification of the paper substrates was successfully performed, showing visible accumulations of the polymer between paper fibers. The distribution of polystyrene on the paper substrates was investigated by SEM on four independently prepared devices. It was observed that the polymer was evenly distributed over the whole paper substrates during modification. Also, the introduction of polystyrene improved hydrophobicity of the paper compared to unmodified paper. As can be seen in Fig. 2, the paper was fully covered by two layers of polystyrene application while there was still gaps between fibers by single layer of polystyrene application. Moreover, three layers of polystyrene modified paper had small gaps, which might be due to over-thickness of the polymer.

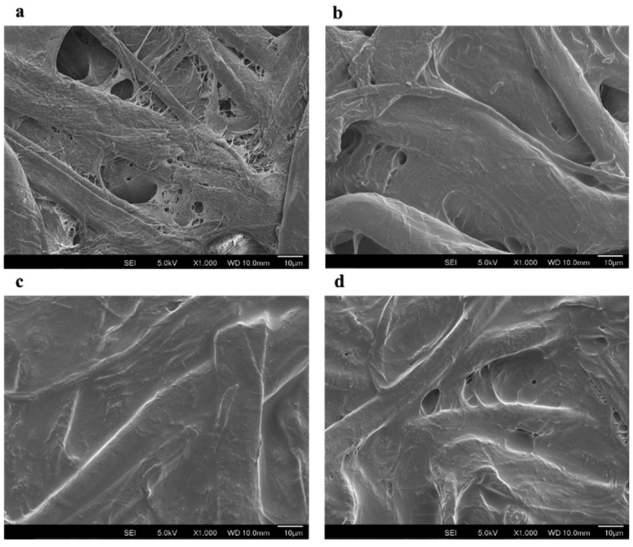

Fig. 2 SEM images of (a) unmodified, (b) one layer, (c) two layers, (d) three layers of polystyrene (0.1 g L^{-1} in dichloromethane) modified paper.

Effect of carbon black nanomaterial on analytical performance of the ISEs

The sensitivity of the device has been improved by increasing nanomaterial layer thickness, preventing the formation of an aqueous layer between the membrane and the electrode substrate.[39–42] The potentiometric responses of K^+-ISE and Na^+-ISE were measured using a portable Wi-Fi-supported potentiostat. The potentiometric signal of K^+-ISE and Na^+-ISE on the dual-ISE-dPAD sensing device increased with the increasing activity of K^+ and Na^+ ions (Fig. 3(a) and (b)). The electrochemical performances of both ISEs are shown in Table 2. The dual-ISE-dPAD demonstrated a sensitivity of 54.14 ± 3.94 mV per decade in the linear range of 0.100 mM to 100 mM K^+ with LOD of 0.05 mM whereas a sensitivity of 55.08 ± 1.15 mV per decade was obtained in the linear range of 5 mM to 1 M Na^+ with LOD of 1.36 mM. Under optimized conditions, Cl^- gave a linear response between 0.50 to 50 mM with a linear equation of $y = 10.489x + 7.0546$ ($R^2 = 0.9937$) (Fig. 4). The LOD and LOQ for Cl^- were found to be 0.16 ± 0.05 mM (3SD) and 0.53 ± 0.05 mM (10SD), respectively.

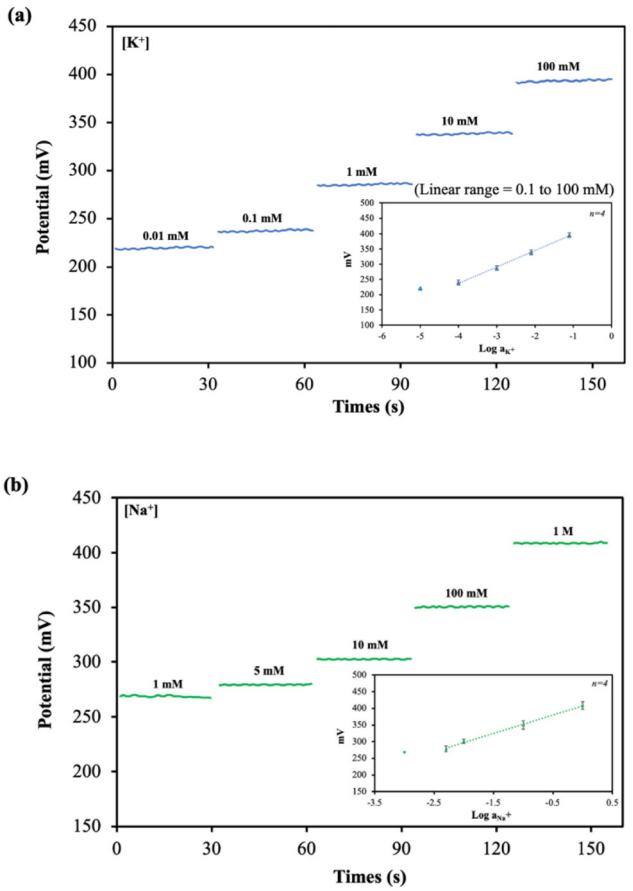

Fig. 3 Potentiometric responses of (a) K^+-ISE and (b) Na^+-ISE to varying activity of K^+ and Na^+ ions, respectively. The inset shows a linear relationship between the potential and the logarithm of (a) K^+ and (b) Na^+ activity in 0.1 M HEPES buffer pH 7.4 (n = 4).

Table 2 Potentiometric response parameters of K^+ and Na^+ (n = 4)

Target ion	Slope (mV per decade)	Intercept (mV)	Linear range (mM)	LOD (mM)
K^+	54.14 ± 3.94	453.07 ± 9.43	0.1 to 100	0.05
Na^+	55.08 ± 1.15	407.60 ± 8.26	5 to 1000	1.36

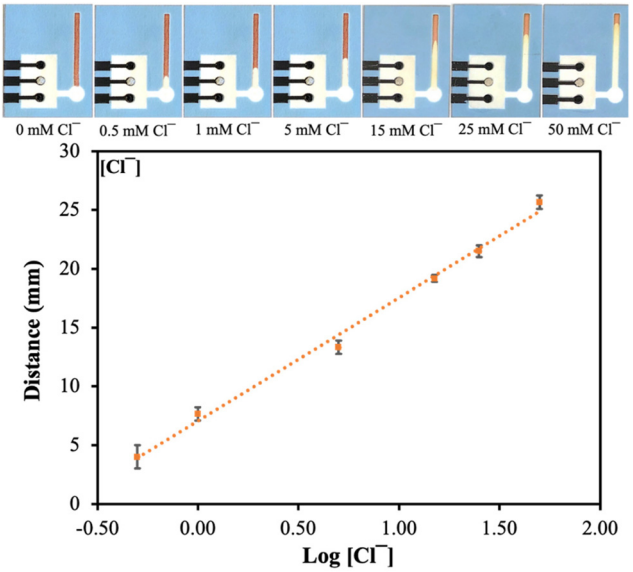

Fig. 4 The figure of a simultaneous device after detected chloride and calibration graph representing the relationship between the logarithm of Cl^- concentration (mM) and color band length (mm) (n = 6).

Carbon black was chosen for modification of the electrode surface to improve sensitivities for K^+ and Na^+ detection. The comparison between carbon black modified and unmodified ISEs was electrochemically studied, and the results are presented in Table S2.† While the slope of K^+-ISE modified with carbon black was 54.16 ± 3.94 mV per decade, it was found as 44.54 ± 3.49 mV per decade for unmodified K^+-ISE. Similarly, the slopes of Na^+-ISE were 55.82 ± 1.15 mV per decade and 38.03 ± 6.78 mV per decade for carbon black modified and unmodified Na^+-ISE, respectively. The data clearly showed that carbon black significantly improved performance of the μPAD in terms of sensitivity. In addition, these results were verified with SEM analysis (Fig. S1†) that carbon black (~100 nm) filled the spaces between TC303 graphite (~20 μm), preventing the formation of aqueous layer between solid contact and plasticized PVC membrane.[43]

Optimization of conditioning time for the ISEs

To achieve a stable signal during potentiometric measurements, the K^+-ISE and Na^+-ISE were conditioned in their primary ion (0.1 M KNO_3 and $NaNO_3$) solutions and the reference electrode was conditioned in 3 M KCl for overnight. Some of the ISEs were left unconditioned for comparison. The response slopes of K^+-ISE and Na^+-ISE conditioned overnight were obtained as 43.81 ± 2.22 mV per decade and 38.42 ± 5.14 mV per decade, respectively (Table S3†). For the ISEs left

unconditioned, the response slopes were 54.16 ± 3.94 mV per decade and 55.82 ± 1.15 mV per decade for K^+-ISE and Na^+-ISE, respectively. Therefore, it was found that both working and reference electrodes left unconditioned gave better response than overnight conditioned ISEs. This is a significant advantage as the device is ready to use for detection of K^+ and Na^+ ions unlike other paper-based ISEs that require a pre-conditioning step (~4–18 h).[25,44]

pH test and response time

The effect of pH was evaluated in the pH range of 2.0–10.0 in the presence of 10 mM K^+ and 10 mM Na^+ (Fig. S2†). The potentiometric signal obtained was constant between pH 2.0 and 8.0 for the K^+-ISE whereas a small drift in the potential response was in the pH range of 8.0–10.0. The potentiometric signal of the Na^+-ISE remained constant from pH 2.0 to 6.0, with a slight potential change in the pH range of 6.0–10.0. The pH effect toward the reaction occurs on dPAD during Cl^- detection was investigated in 20 mM Cl^- in the pH range of 2.0 to 10.0.[28] According to Fig. S5,† it was observed that the Cl^- detection on dPAD was not affected by change in pH of the analyte. Therefore, the sensing device has wide working pH range, providing suitability for the use in clinical applications. To determine the response time, the average time necessary for the dual-ISE to reach a potential response within 1.0 mV of the final equilibrium EMF value obtained by consecutive immersion of tenfold increased concentrations of the primary ion solution (K^+ or Na^+) was recorded.[45] The potentiometric response time is approximately 30 s for both K^+-ISE and Na^+-ISE.

Selectivity of the assay

The selectivity of the electrodes was tested in the presence of the interferents consisting of 100 mM of Ca^{2+}, Mg^{2+}, PO_4^{3-}, CO_3^{2-}, D-glucose, and urea, mixed with 10 mM of K^+ or 10 mM Na^+ (The concentration less than ions interferes 10 times) primary ions, respectively. As shown in Fig. S3(a) and (b),† the other ions did not affect the potentiometric responses of both K^+-ISE and Na^+-ISE. Therefore, the developed ISE-K^+–Na^+ can selectively measure K^+ and Na^+ in the presence of interfering ions.

In addition, the logarithmic selectivity coefficients were calculated using the Nicolskii–Eisenman equation: $\log_{I,J}^{pot} = \frac{(E_J - E_I)Z_I F}{2.303RT} + \log\frac{a_I}{a_J^{Z_i/Z_j}}$ (E_I and E_J represent the potential value of target ions and interfering ions, respectively; a_I and a_J represent the activity of target ions and interfering ions, respectively; Z_I and Z_J represent the charge number of target ions and interfering ions, respectively).[22] The interfering effect was tested using the separate solution method in 1 mM targets analyte and interfering ions and, calculated by the Nicolskii–Eisenman equation.[46] The $\log_{K^+,J}^{pot}$ and $\log_{Na^+,J}^{pot}$ tested by our device are presented in the Table 3. Consequently, our dual-ISE shows high selectivity for K^+ and Na^+ in the presence of various interferents.

Table 3 Logarithmic selectivity coefficients of sensing channels in the dual-ISE (n = 4)

Interfering ions	$\log_{K^+,J}^{pot}$	$\log_{Na^+,J}^{pot}$
K^+	—	−2.74 ± 0.16
Na^+	−3.59 ± 0.11	—
Ca^{2+}	−3.44 ± 0.08	−3.83 ± 0.08
Mg^{2+}	−2.90 ± 0.14	−3.51 ± 0.07
PO_4^{3-}	−2.90 ± 0.12	−2.85 ± 0.12
CO_3^{2-}	−3.20 ± 0.08	−3.24 ± 0.14

The selectivity of dPAD was determined by testing the response of the assay to 20 mM Cl^- in the presence of interfering ions, including 100 mM of Ca^{2+}, Mg^{2+}, PO_4^{3-}, CO_3^{2-}, glucose, urea, Na^+, and K^+.[28] The results indicated that the Cl^- signal was not affected with these ions by an error of 10% (Fig. S6†).

Water layer test

The presence of a water layer formation between the PVC membrane and the solid-state contact was also studied. K^+-ISE was measured in 0.1 M K^+ solution for 30 min and then exposed to 0.1 M Na^+ as an interfering ion for 30 min, followed by 0.1 M of the K^+ solution again (Fig. S4(a)†). In a similar condition, potentiometric response of the Na^+-ISE was measured in 0.1 M Na^+ solution for 30 min and then 0.1 M K^+ as an interfering ion for 30 min followed by 0.1 M of the Na^+ solution (Fig. S4(b)†). K^+-ISEs exhibited a potential drift when Na^+ was introduced to the electrode due to the diffusion of K^+ to the membrane layer. Once the electrodes were returned to the K^+ solution, the initial value was obtained, demonstrating the lack of a water layer at the ion-selective membrane/carbon black-ePAD interface. The carbon black was used to increase hydrophobicity between the PVC membrane and solid contact.[47] Although this sensing device was aimed for single-use for urine analysis, these results confirms that the ePAD part could be used for continuous monitoring of analytes.

Reproducibility and shelf life

The reproducibility of dual-ISE-PAD was tested using 10 separate electrodes, and their average standard potentials $E°$ were calculated by extrapolating the linear response of the ISEs where the primary ion concentration is equal to 1 M.[48] The relative standard deviations (RSDs) were found to be 5.01% and 2.71% for K^+-ISE and Na^+-ISE, respectively (Table S4†), showing excellent reproducibility. The shelf life of the dual-ISE-PAD was investigated over eight weeks by measuring the response slope for K^+-ISE and Na^+-ISE and percent recovery for Cl^- detection on dPAD and presented in Table S5.† The device was stored in dark and dry conditions when not in use. The observed slopes changed from 52.85 ± 2.65 mV per decade to 51.57 ± 1.51 mV per decade and from 52.10 ± 1.41 mV per decade to 52.05 ± 1.58 mV per decade for K^+-ISE and Na^+-ISE while the percent recovery of Cl^- was 95 ± 4%, showing that

Table 4 Detection of K^+ and Na^+ in sample with the ISE and Detection of Cl^- with the dPAD (n = 6)

			ISE	
Sample	Analyte	[Spike] (mM)	Found (mM)	%Recovery
Urine	K^+	0	4.82 ± 0.51	—
		25	27.43 ± 2.90	90
		125	121.40 ± 9.66	93
		340	371.63 ± 21.50	108
	Na^+	0	52.19 ± 5.72	
		40	89.87 ± 4.25	94
		110	167.58 ± 11.32	105
		440	516.36 ± 20.34	105
			dPAD	
Sample	Analyte	[Spike] (mM)	Found (mM)	%Recovery
Urine	Cl^-	0	35.34 ± 4.34	—
		25	57.83 ± 5.83	90
		125	149.13 ± 16.83	91
		340	363.20 ± 50.87	96

the device has high stability and a long shelf life. The results show that both detection parts of the hybrid device were stable over eight weeks.

Sample analysis

After the device was electrochemically and physically characterized, the applicability of the dual ISE-dPAD was verified by the standard addition method in normal urine samples. The urine sample was spiked with the standard K^+ (0, 25, 125, and 340 mM), Na^+ (0, 40, 110, and 440 mM), and Cl^- (0, 25, 125, and 340 mM), and diluted 20 times with 0.1 M HEPES buffer solution pH 7.4 before measurements. The standard and calculated concentration results based on calibration curves are demonstrated in Table 4. Our device presented the percent recoveries of K^+, Na^+, and Cl^- of 90–108%, 94–105%, and 90–96%, respectively. These recovery values suggested that this method is reliable according to the Official Food and Drug Administration (FDA) recommendations.[49] The presented sensing device represents the potential for developing at-home electrolyte detection.

Conclusions

We engineered the paper substrate to fabricate a dual-mode μPAD for potentiometric and colorimetric detection. The paper material is suitable for the biomedical samples due to its cost-effectiveness and disposability. The non-ionic polymer coated paper was used to develop ISEs for simultaneous detection of K^+ and Na^+. Two layers of polymer coating on paper gave the best sensitivity for the ISEs. Moreover, we exploited the combination of dPAD for colorimetric determination of Cl^-. The K^+-ISE channel gave a potentiometric response of 54.14 ± 3.94 mV per decade in a concentration range of 0.100 mM to 100 mM, with a LOD of 0.05 mM while the Na^+-ISE had a response of 55.08 ± 1.15 mV per decade in a linear concentration range of 5 mM to 1 M with a LOD of 1.36 mM. The dual-ISE-dPAD was applied to detect K^+, Na^+, and Cl^- in spiked human pooled urine and the recoveries were 90–108%, 94–105%, and 90–96%, respectively, which is in good agreement. Our proposed assay offers low-cost, sensitive, simultaneous and rapid analysis of K^+, Na^+, and Cl^- ions on a single device for biological samples. Due to their single-use, the device is not subject to biofouling and could be readily used without the need of pre-conditioning step. This dual-mode device could be easily adapted for other biomedically or environmentally relevant ions in the future.

Author contributions

Dr Kamonchanok Phoonsawat: conceptualization, methodology, investigation, writing – original draft. Dr Tugba Ozer: conceptualization, methodology, supervision, project administration, funding acquisition, writing – review & editing. Dr Wijitar Dungchai: supervision, funding acquisition. Dr Charles S. Henry: conceptualization, supervision, writing – review & editing, project administration, funding acquisition.

Conflicts of interest

There are no conflicts to declare.

Acknowledgements

The authors gratefully acknowledge financial support from the Petchra Pra Jom Klao Ph.D. Research Scholarship, Innovation and Partnerships Office, King Mongkut's University of Technology Thonburi, Thailand. This work was also financially supported by The Scientific and Technological Research Council of Turkey (TUBITAK, Project No. 120N615), Turkey and Colorado State University, USA.

References

1 M. Umbrello, P. Formenti and D. Chiumello, *Anesth. Analg.*, 2020, **131**(5), 1456–1470.
2 F. Ghaderinezhad, H. Ceylan Koydemir, D. Tseng, D. Karinca, K. Liang, A. Ozcan and S. Tasoglu, *Sci. Rep.*, 2020, **10**, 13620.
3 A. J. Viera and N. Wouk, *Am. Fam. Physician*, 2015, **92**, 487–495.
4 J. H. Ix and C. A. M. Anderson, *J. Am. Med. Assoc.*, 2018, **319**, 1201–1202.
5 P. Mirmiran, Z. Gaeini, Z. Bahadoran, A. Ghasemi, R. Norouzirad, M. Tohidi and F. Azizi, *Eur. J. Med. Res.*, 2021, **26**, 3.
6 N. R. Cook, E. Obarzanek, J. A. Cutler, J. E. Buring, K. M. Rexrode, S. K. Kumanyika, L. J. Appel, P. K. Whelton

and T. o. H. P. C. R. Group, *Arch. Intern. Med.*, 2009, **169**, 32–40.
7 V. Perez and E. T. Chang, *Adv. Nutr.*, 2014, **5**, 712–741.
8 Q. Yang, T. Liu, E. V. Kuklina, W. D. Flanders, Y. Hong, C. Gillespie, M.-H. Chang, M. Gwinn, N. Dowling, M. J. Khoury and F. B. Hu, *Arch. Intern. Med.*, 2011, **171**, 1183–1191.
9 C. A. Grimes, J. R. Baxter, K. J. Campbell, L. J. Riddell, M. Rigo, D. G. Liem, R. S. Keast, F. J. He and C. A. Nowson, *JMIR Res. Protoc.*, 2015, **4**, e7–e7.
10 E. N. Kapinus, I. A. Revelsky, V. O. Ulogov and Y. A. Lyalikov, *J. Chromatogr. B: Anal. Technol. Biomed. Life Sci.*, 2004, **800**, 321–323.
11 L. B. d. Caland, E. L. C. Silveira and M. Tubino, *Anal. Chim. Acta*, 2012, **718**, 116–120.
12 H. Chen, Y.-S. Gal, S.-H. Kim, H.-J. Choi, M.-C. Oh, J. Lee and K. Koh, *Sens. Actuators, B*, 2008, **133**, 577–581.
13 J. Nelson, L. Poirier and F. Lopez-Linares, *J. Anal. At. Spectrom.*, 2019, **34**, 1433–1438.
14 R. Paulauskas, N. Striūgas, M. Sadeckas, P. Sommersacher, S. Retschitzegger and N. Kienzl, *Sci. Total Environ.*, 2020, **746**, 141162.
15 T. Ozer, C. McMahon and C. S. Henry, *Annu. Rev. Anal. Chem.*, 2020, **13**, 85–109.
16 E. Noviana, T. Ozer, C. S. Carrell, J. S. Link, C. McMahon, I. Jang and C. S. Henry, *Chem. Rev.*, 2021, **121**, 11835–11885.
17 N. Ruecha, O. Chailapakul, K. Suzuki and D. Citterio, *Anal. Chem.*, 2017, **89**, 10608–10616.
18 J. Bobacka, A. Ivaska and A. Lewenstam, *Chem. Rev.*, 2008, **108**, 329–351.
19 A. Lynch, D. Diamond and M. Leader, *Analyst*, 2000, **125**, 2264–2267.
20 B. Schazmann, D. Morris, C. Slater, S. Beirne, C. Fay, R. Reuveny, N. Moyna and D. Diamond, *Anal. Methods*, 2010, **2**, 342–348.
21 T. Ozer and C. S. Henry, *Microchim. Acta*, 2022, **189**, 152.
22 F. Wang, Y. Liu, M. Zhang, F. Zhang and P. He, *Anal. Chem.*, 2021, **93**, 8318–8325.
23 Q. Cao, B. Liang, X. Mao, J. Wei, T. Tu, L. Fang and X. Ye, *Electroanalysis*, 2021, **33**, 643–651.
24 W.-J. Lan, X. U. Zou, M. M. Hamedi, J. Hu, C. Parolo, E. J. Maxwell, P. Bühlmann and G. M. Whitesides, *Anal. Chem.*, 2014, **86**, 9548–9553.
25 R. Ding, N. K. Joon, A. Ahamed, A. Shafaat, M. Guzinski, M. Wagner, T. Ruzgas, J. Bobacka and G. Lisak, *Sens. Actuators, B*, 2021, **344**, 130200.
26 W. A. Ameku, J. M. Goncalves, V. N. Ataide, M. S. Ferreira Santos, I. G. Gutz, K. Araki and T. R. Paixão, *ACS Omega*, 2021, **6**, 594–605.
27 P. Rattanarat, W. Dungchai, D. Cate, J. Volckens, O. Chailapakul and C. S. Henry, *Anal. Chem.*, 2014, **86**, 3555–3562.
28 K. Phoonsawat, I. Agir, W. Dungchai, T. Ozer and C. S. Henry, *Anal. Chim. Acta*, 2022, 340245.
29 Y. Soda, H. Shibata, K. Yamada, K. Suzuki and D. Citterio, *ACS Appl. Nano Mater.*, 2018, **1**, 1792–1800.
30 S. Papp, G. Jágerszki and R. E. Gyurcsányi, *Angew. Chem., Int. Ed.*, 2018, **57**, 4752–4755.
31 K. Pungjunun, A. Yakoh, S. Chaiyo, N. Praphairaksit, W. Siangproh, K. Kalcher and O. Chailapakul, *Microchim. Acta*, 2021, **188**, 1–11.
32 T. Ozer, I. Agir and C. S. Henry, *Sens. Actuators, B*, 2022, **365**, 131961.
33 T. Ozer, I. Agir and C. S. Henry, *Talanta*, 2022, 123544.
34 J. Sutter, A. Radu, S. Peper, E. Bakker and E. Pretsch, *Anal. Chim. Acta*, 2004, **523**, 53–59.
35 R. B. Channon, M. P. Nguyen, A. G. Scorzelli, E. M. Henry, J. Volckens, D. S. Dandy and C. S. Henry, *Lab Chip*, 2018, **18**, 793–802.
36 M. Rahbar, B. Paull and M. Macka, *Anal. Chim. Acta*, 2019, **1063**, 1–8.
37 R. Ottewill and R. Satgurunathan, *Colloid Polym. Sci.*, 1987, **265**, 845–853.
38 J. Bobacka, *Anal. Chem.*, 1999, **71**, 4932–4937.
39 T. Ozer and C. S. Henry, *Electrochim. Acta*, 2022, **404**, 139762.
40 M. Parrilla, M. Cuartero, S. Padrell Sánchez, M. Rajabi, N. Roxhed, F. Niklaus and G. A. Crespo, *Anal. Chem.*, 2019, **91**, 1578–1586.
41 T. Ozer and C. S. Henry, *Microchim. Acta*, 2022, **189**, 1–12.
42 T. Ozer, *Anal. Sci.*, 2022, 1–11.
43 B. Paczosa-Bator, *Talanta*, 2012, **93**, 424–427.
44 V. Mazzaracchio, A. Serani, L. Fiore, D. Moscone and F. Arduini, *Electrochim. Acta*, 2021, **394**, 139050.
45 C. Maccà, *Anal. Chim. Acta*, 2004, **512**, 183–190.
46 E. Bakker, E. Pretsch and P. Bühlmann, *Anal. Chem.*, 2000, **72**, 1127–1133.
47 M. Pięk, B. Paczosa-Bator, J. Smajdor and R. Piech, *Electrochim. Acta*, 2018, **283**, 1753–1762.
48 M. A. Arnold and M. E. Meyerhoff, *Anal. Chem.*, 1984, **56**, 20–48.
49 U. FDA, *US Department of Health and Human Services Food and Drug Administration Center for Drug Evaluation and Research and Center for Veterinary Medicine*, 2018.